PHILOSOPHICAL TRANSACTIONS OF THE ROYAL SOCIETY A

Phil. Trans. R. Soc. A (2005) **363**, 1551–1571
doi:10.1098/rsta.2005.1595
Published online 1 July 2005

Rapid motions of free-surface avalanches down curved and twisted channels and their numerical simulation

By Shiva P. Pudasaini, Yongqi Wang and Kolumban Hutter

Department of Mechanics—AG III, Darmstadt University of Technology, Hochschulstrasse 1, 64289, Darmstadt, Germany
(pudasain@mechanik.tu-darmstadt.de)

This paper presents a new model and discussions about the motion of avalanches from initiation to run-out over moderately curved and twisted channels of complicated topography and its numerical simulations. The model is a generalization of a well established and widely used depth-averaged avalanche model of Savage & Hutter and is published with all its details in Pudasaini & Hutter (Pudasaini & Hutter 2003 *J. Fluid Mech.* **495**, 193–208). The intention was to be able to describe the flow of a finite mass of snow, gravel, debris or mud, down a curved and twisted corrie of nearly arbitrary cross-sectional profile. The governing equations for the distribution of the avalanche thickness and the topography-parallel depth-averaged velocity components are a set of hyperbolic partial differential equations. They are solved for different topographic configurations, from simple to complex, by applying a high-resolution non-oscillatory central differencing scheme with total variation diminishing limiter. Here we apply the model to a channel with circular cross-section and helical talweg that merges into a horizontal channel which may or may not become flat in cross-section. We show that run-out position and geometry depend strongly on the curvature and twist of the talweg and cross-sectional geometry of the channel, and how the topography is shaped close to run-out zones.

Keywords: rapid granular avalanches; free-surface motion; natural terrains; curved and twisted channels; hyperbolic equations; numerical simulation

1. Introduction

Natural hazards such as avalanches, debris- and mud-flows as well as landslides are common natural phenomena to the inhabitants of high-mountain areas. People and municipal authorities in these areas who have learned to accept their occasional occurrence and to avoid the damage that accompanies them are always seeking to minimize such unpleasant and sometimes unavoidable happenings, causing the death and damage of the life and property of the people. In the second half of the last century, significant efforts were undertaken to understand the mechanisms of formation of avalanches at high elevations, dynamics of the motion along the complicated and non-trivial mountain tracks

One contribution of 11 to a Theme 'Geophysical granular and particle-laden flows'.

and settlements of such huge and catastrophic events in the flat valleys. Special attention was paid to the mechanical, dynamical and the geometrical parts of the problem. Several theories were proposed, ranging from statistical and mass point models to hydraulic and molecular dynamics formulations including the kinetic theories. Of the abundant number of papers, we mention Lied & Bakkehøi (1980), McClung & Lied (1987) and Lied & Toppe (1989) for the statistical approach, Voellmy (1955), Salm (1966) and Perla *et al.* (1980) for the mass point models, Grigoryan & Ostroumov (1977) and Eglit (1983) for the hydraulic models, Savage (1989) for the molecular dynamics approach and Jenkins (2001) for a hydraulic model using the kinetic theory. The subject has been reviewed in parts by Hutter & Rajagopal (1994) and Hutter (1996), and an attempt to list (almost) all available snow avalanche models was made in the SAME (Snow Avalanche Modelling, Mapping and Warning in Europe) report (Harbitz 1998). Complementary information on debris flow and flow from volcanic eruptions is given by Iverson & Denlinger (2001), Denlinger & Iverson (2001, 2004), Pitman *et al.* (2003), Iverson *et al.* (2004) and Patra *et al.* (in press). Different numerical techniques were developed and well implemented, and a number of experiments both in the laboratory and the field were performed. Here, mention might be made of Hutter and others (e.g. Hutter 1996), Keller *et al.* (1998), Iverson & Denlinger (2001) and Iverson *et al.* (2004) for laboratory and out-door experiments and Gubler (1987), Norem *et al.* (1987) and Zwinger *et al.* (2003) for the collection of field data, reviewed for snow by Issler (2003). As for numerical methods, we mention Denlinger & Iverson (2001, 2004), Tai *et al.* (2002), Koschdon & Schäfer (2003), Vollmöller (2004) and Patra *et al.* (in press). The aim behind these scientific and technical activities is to forecast the occurrence of avalanches and debris flows and to predict zones of encounters either on their tracks or down in the valley as they come to settlements. This will eventually merge into the construction of hazard maps, classifying the regions as dangerous, less dangerous and danger-free zones. Nevertheless, accidents causing damage of property and loss of life have regularly occurred in the past and continue to occur today. This points at the need of research of avalanches and debris flows at intensified levels, and makes it a topic of permanent public concern in mountainous regions.

Since avalanches and debris flows in natural terrain are geometrically complex, their prediction of flow path and deposition, including the design of defence measures, are difficult and fraught with large errors. To reduce, these and to restrict them as far as possible to the truly statistical causes, model parts, which can be based on deterministic prerequisites, ought to be described as accurately as possible. Such efforts have been the focus in the last few years, and the above-mentioned literature mirrors this state. By and large, efforts concentrated on rigorous descriptions of the motion of a finite mass of snow, soil or debris down a prescribed topography using deterministic classical physics and its mathematical-numerical exploitation and leaving the statistics to the uncertainties of the exact prediction, initial and boundary data and the phenomenological parameters through error-fraught validation procedures.

In this paper, we use a new set of model equations and present discussions regarding the motion of avalanches from initiation to run-out down mountain valleys or corries that are curved and twisted. Ideally, the motion ought to be channelized, however the fission into two channels from a single one is in principle thinkable if undoubtedly very complex. The model has been presented by Pudasaini & Hutter (2003) and only its salient parts will be given here, as our focus will be on the presentation of numerical results of flows of a finite mass of a granular material down idealized channels with curvature and torsion and topographic variations. Cross-sections and talwegs will be varied so as to allow us to scrutinize the reaction of the moving piles to curvature and torsion effects as well as variations in the topography close to the run-out zone. Comparison with laboratory data and application to natural topographies are not yet ready.

The model equations are solved by implementing the non-oscillatory central (NOC) scheme with total variation diminishing (TVD) limiters (see Nessyahu & Tadmor 1990; Jiang & Tadmor 1998). These are high-resolution numerical techniques able to resolve the steep height and velocity gradients and moving sharp fronts that are often observed in experiments and field events but not captured by traditional finite-difference schemes. Our numerical technique is based on Wang *et al.* (2004) and uses NOC schemes with an optimal limiter. We performed several numerical tests for avalanching masses down curved and twisted bed topographies (Pudasaini 2003). Uniformly and non-uniformly curved and twisted channels as well as channels which incorporate continuous transition zones merging into the horizontal run-out zones are considered. Channels with both confined and unconfined transition zones, with constant and variable inclination angles of the topography, are studied. The results demonstrate a sensitive reaction of the flow of the granular mass to the variations in curvature, twist and the topography. In particular, the peculiarities of the quantities in the transition zone immediately before the entrance of the avalanche into the run-out region. They demonstrate that not only the run-out distance but also the sidewise position of the final deposit depend crucially on how the curvature and twist of the talweg behave individually and together as the avalanche track enters the run-out zone.

2. Model equations

Before presenting the model equations proposed by Pudasaini & Hutter (PH; 2003), we briefly discuss the physically justified and realistic assumptions made in the development of the model equations. Savage & Hutter (SH; 1989) developed a hydraulic theory for flows in vertical planes to describe the evolving geometry of a finite mass of a granular material and the associated velocity distribution as an avalanche slides down an inclined chute. In order to formulate a realistic model, the following assumptions were made: (i) the moving dry and cohesionless granular mass is incompressible and obeys a Mohr–Coulomb yield criterion both inside the deforming mass as well as at the sliding basal surface. (ii) The geometries of the avalanching masses are shallow in the sense that typical avalanche thicknesses are small in comparison to the extent parallel to the sliding surface. (iii) To obtain a dimensionally reduced theory, the field equations are integrated through the depth of the pile, and a nearly uniform velocity profile through the depth is assumed. (iv) Scaling analysis identifies the physically significant terms in the equations and isolates those that can be neglected. These assumptions are supported by observations of large-scale snow avalanches in the fields as well as small-scale laboratory avalanches of different dry granular particles sliding and deforming down different chutes and channels. These facts are well documented and can be found in the literature (Savage & Hutter 1989; Hutter & Koch 1991; Dent *et al.* 1998; Keller *et al.* 1998; McElwaine & Nishimura 2001; Pudasaini 2003; Ancey & Meunier 2004; Denlinger & Iverson 2004; Hutter *et al.* 2004; Iverson *et al.* 2004). The simple spatially one-dimensional model of SH, applicable along a straight chute, has been generalized to higher dimensions, to more complex geometries, and has been tested against realistic laboratory experiments and back calculations of the field events. Good to excellent agreements were obtained between the theoretical predictions and the experiments and field data. For a review of own work, see Hutter *et al.* (2004), but also the SAME report by Harbitz (1998), and Denlinger & Iverson (2004), Pitman *et al.* (2003) and Patra *et al.* (in press). Here we will focus on a recent three-dimensional extension of the SH model by PH and its application to avalanche motion over a realistic three-dimensional flow path as pointed out earlier.

(*a*) *Effects of the topography*

Curved flow-path surfaces strongly influence the flow dynamics because transverse shearing and cross-stream momentum transport occur when the topography obstructs or redirects the motion due to its curvature and torsion. Local deceleration and deposition of mass may occur due to energy dissipation. Resistance due to basal friction is modified by 'centrifugal forces' induced by bed curvature and torsion.

Recently, Pudasaini & Hutter (2003) extended the SH theory to flows of dry granular masses in a *non-uniformly curved and twisted channel*. Consider an avalanche-prone landscape and a subregion of it where the topography allows identification of the likely avalanche track. A space curve parallel to the talweg of the valley is singled out as a master curve, C (which can be obtained, for example, by shifting the talweg along its normal direction), from which the track topography will be modelled. The curvature and torsion of the master curve $\kappa=\kappa(x)$, $\tau=\tau(x)$, are either assumed to be known or can be computed from digital elevation geographic information systems (GIS) data as functions of the arc length x of the master curve. Then, an orthogonal coordinate system along the master curve is introduced and the model equations are derived in this general coordinate system. In the model equations of this paper, (x, y) form a curved reference surface, where x is the coordinate along the talweg of a mountain valley, while y is the circular arc length in a cross-sectional plane perpendicular to the talweg of which the value is determined by the relation $y=\varepsilon\theta z_{\mathrm{T}}$, where ε is the aspect ratio between the avalanche height and the extent, θ is the azimuthal angle which accounts for the cross-slope curvature and z_{T} (usually $z_{\mathrm{T}}\gg 1$) is the radial distance between the master curve and the talweg and z is the coordinate perpendicular to the reference topography. Every quantity in this paper is written in non-dimensional form. The channel topography and the geometry of the avalanche in the lateral and longitudinal directions are illustrated in figure 1. Let us discuss some terms and parameters arising in the model equations presented in the §2*b*. g_x, g_y and g_z are the projected components of the gravitational acceleration along the down-slope, cross-slope and normal

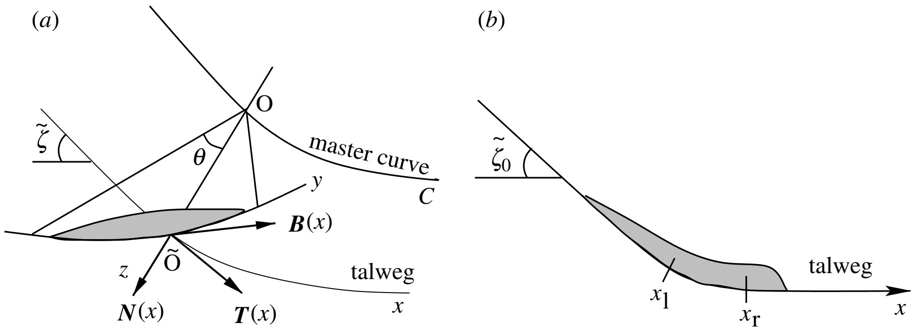

Figure 1. (a) the avalanche domain in the lateral direction occupies a region in a circular section of a plane perpendicular to the talweg of the valley and θ is the azimuthal angle in this plane. $O\tilde{O}=z_{\mathrm{T}}$ is the radial distance between the master curve and the talweg. $\{\boldsymbol{T}, \boldsymbol{N}, \boldsymbol{B}\}$ is the moving orthonormal unit triad following the talweg. $\tilde{\zeta}$ is the slope angle of the talweg with the horizontal. The depth of the avalanche in this section is represented by a height function $h(x, y, t)$ and is measured in the radial direction. (b) avalanche passing through the transition into the run-out zone in a vertical plane containing the talweg of the valley. In this picture, x_{l} and x_{r} are the left and right end points of the continuous transition between the straight inclined upper part with inclination angle $\tilde{\zeta}_0$ and the horizontal run-out in the valley.

directions, for explicit computation see Pudasaini & Hutter (2003). The aspect ratio ε, and the measure of curvature relative to the typical avalanche length, λ, are both small numbers. The basal topography (which is the deviation of the basal topography from the reference surface $z=0$, and includes the small-scale geometric features of the bed topography) will be denoted by $z=b(x, y)$.

The theory is designed to model the flow of (debris) avalanches over channels having general curvature and torsion. Although there are other models that consider the problem of avalanche motion over curved slopes (e.g. Maeno & Nishimura 1987; Norem *et al.* 1987; Savage & Nohguchi 1988; Zwinger *et al.* 2003; Iverson *et al.* 2004; Pitman *et al.* 2003; see also the SAME report edited by Harbitz 1998), the model equations considered in this paper are the first to explicitly include curvature and torsion effects in a systematic manner. This makes the extended model amenable to realistic snow and debris motions down arbitrary guiding topographies. In fact, GIS data of mountains avalanche- and debris-prone regions can be implemented to this model, which provides the geometrical basis for realistic application. In contrast to the original SH theory and all their previous extensions (e.g. Gray *et al.* 1999; Pudasaini *et al.* 2003a,b), *a moderately curved and twisted space curve* is used to define an orthogonal curvilinear coordinate system. The final governing balance laws of mass and momentum are written in these coordinates.

(b) *Description of the model equations*

As in the previous models of the SH-theory, Pudasaini & Hutter (2003) formulated the balance laws of mass and momentum as well as the boundary conditions in slope-fitted curvilinear coordinates of mountain surfaces, averaged these equations over depth, and then non-dimensionalized the equations. The final balance laws of mass, and momentum in the down-slope and cross-slope directions, take the forms

$$\frac{\partial h}{\partial t} + \frac{\partial}{\partial x}(hu) + \frac{\partial}{\partial y}(hv) = 0, \tag{2.1}$$

$$\frac{\partial}{\partial t}(hu) + \frac{\partial}{\partial x}(hu^2) + \frac{\partial}{\partial y}(huv) = hs_x - \frac{\partial}{\partial x}\left(\frac{\beta_x h^2}{2}\right), \tag{2.2}$$

$$\frac{\partial}{\partial t}(hv) + \frac{\partial}{\partial x}(huv) + \frac{\partial}{\partial y}(hv^2) = hs_y - \frac{\partial}{\partial y}\left(\frac{\beta_y h^2}{2}\right), \tag{2.3}$$

where h is the depth of the avalanche measured normal to the reference surface and the factors β_x and β_y are defined as

$$\beta_x = -\varepsilon g_z K_x, \quad \beta_y = -\varepsilon g_z K_y. \tag{2.4}$$

The terms s_x and s_y represent, respectively, the net driving accelerations in the down-slope and cross-slope directions and are given by

$$s_x = g_x - \frac{u}{|\boldsymbol{u}|}\tan\delta(-g_z + \lambda\kappa\eta u^2) + \varepsilon g_z \frac{\partial b}{\partial x}, \tag{2.5}$$

$$s_y = g_y - \frac{v}{|\boldsymbol{u}|}\tan\delta(-g_z + \lambda\kappa\eta u^2) + \varepsilon g_z \frac{\partial b}{\partial y}, \tag{2.6}$$

$|\boldsymbol{u}| = \sqrt{u^2 + v^2}$ is the magnitude of the velocity field tangential to the reference (basal) topography. Similarly, $\lambda\kappa$ is the local radius of curvature of the talweg, while

$$\eta = \cos(\theta + \varphi(x) + \varphi_0), \tag{2.7}$$

where $\varphi(x) = -\int_{x_0}^{x} \tau(x')\mathrm{d}x'$ gives the accumulation of the torsion of the talweg from an initial position x_0 and φ_0 (here, $\varphi_0 = -\pi/2$ is considered) is a constant.

The first terms on the right-hand side of (2.5) and (2.6) are the gravitational accelerations in the down- and cross-slope directions, respectively. The second terms represent the dry Coulomb friction in which the normal tractions comprise the overburden pressure (g_z), plus a contribution due to the curvature and torsion of the master curve ($\lambda\kappa\eta u^2$). Finally, the third terms are the projections of the topographic variations along the normal direction. K_x and K_y in equation (2.4) are called the earth pressure coefficients. Elementary geometrical arguments and Mohr's circles may be used to determine these values as functions of the internal (ϕ) and basal (δ) angles of friction (Hutter *et al.* 1993, 2005), i.e.

$$\left.\begin{aligned} K_x &= K_{x_{\mathrm{act/pass}}} = 2\sec^2\phi\left(1 \mp \sqrt{1 - \cos^2\phi\sec^2\delta}\right) - 1, \qquad (\partial u/\partial x) \gtrless 0, \\ K_y &= K_{y_{\mathrm{act/pass}}} = \frac{1}{2}\left(K_x + 1 \mp \sqrt{(K_x - 1)^2 + 4\tan^2\delta}\right), \quad (\partial v/\partial y) \gtrless 0, \end{aligned}\right\} \tag{2.8}$$

where K_x and K_y are active during dilatational motion (upper sign) and passive during compressional motion (lower sign). We note that ignoring the $O(\varepsilon)$-contributions in (2.1)–(2.6) reduces the equations to a point mass model and does not allow the deformation of the pile to be determined. We also claim, in disagreement with recent alternative version of these equations for torsion-free master curves, presented by Gray *et al.* (2003), that the distinction between active and passive state of stresses is physically significant.

Given the master curve, C, the material parameters δ and ϕ and the elevation of the basal topography, b, above the curved reference surface, equations (2.1)–(2.3) allow h, u and v to be computed as functions of space and time, once appropriate initial and boundary conditions are prescribed, where h is the avalanche depth, and (u, v) are the depth-averaged velocity components parallel to the flow surface. As an initial condition, one commonly prescribes the geometry and velocity distributions of the avalanche at the initial time, usually for a mass at rest. The boundary is defined as those locations where the avalanche height goes to zero.

(*c*) *Comparison with previous models*

Equations (2.1)–(2.3) constitute a *two-dimensional conservative system of equations* that entails several advantages over previous model equations. They are as follows. (i) The equations simultaneously include the curvature and torsion of the channelized basal topography. Therefore, they can be utilized to describe the flow of avalanches along non-uniformly curved and twisted channels. (ii) There is a non-zero gravity term g_y in the cross-slope direction that takes into account the global effect of topographic variation in the lateral direction. Thus, the lateral motion is explicitly gravity driven, not indirectly via lateral pressure gradients. This might be very crucial in designing defence structures and when dealing with the motion of avalanches that hit obstructions or deflecting structures on their way. The torsion effect η of the topography is included in the net driving force components s_x and s_y in the two flow directions. The components of the gravitational acceleration also depend on both the curvature and the torsion of the basal topography (see Pudasaini & Hutter 2003). The y-coordinate, which was just a straight line before, is now curved in the cross-slope direction and for a torsion-free master curve, which lies in a vertical plane, these model equations exactly reproduce all previous extensions of the SH equations as special cases (for a proof, see Pudasaini & Hutter 2003; Pudasaini 2003). (iii) We can form a three-dimensionally curved and twisted channel using down-slope and cross-slope coordinates x and y. In principle, it is thus possible to model a given channel or avalanche gully by considering its talweg and by choosing θ appropriately as a function of the down- and cross-slope coordinates. These are considerably new flexibilities of the model equations that are crucial to describe the motion of avalanching debris flows in curved and twisted channels and mountain terrains in a more realistic manner.

3. Numerical techniques

The avalanche equations (2.1)–(2.3) comprise a *nonlinear hyperbolic system*. Shock formation is an essential mechanism in granular flows on an inclined surface merging into a horizontal run-out zone or encountering an obstacle when the velocity becomes subcritical from its supercritical state. To produce more accurate and physically reliable solutions of strongly convective nonlinear hyperbolic equations, it is therefore natural to apply conservative high-resolution numerical techniques that are able to resolve the steep gradients of the unknown variables and moving fronts often observed in experiments and field events of avalanches. The NOC scheme proposed first by Nessyahu & Tadmor (1990) and extended to higher dimensions by Jiang & Tadmor (1998) is implemented to solve the model equations. This is a high-resolution shock capturing scheme. The necessary background and full details of this method can be found in the literature (e.g. Harten 1983; Harten *et al.* 1986; Yee 1987; Nessyahu & Tadmor 1990; LeVeque 1990; Kröner 1997; Jiang & Tadmor 1998; Toro 2001) and its application to avalanches is given by Tai (2000), Tai *et al.* (2002), Pudasaini (2003) and Pudasaini *et al.* (2004).

Essentially, this scheme requires the system to be written in terms of conservative variables, which are the avalanche thickness, h and the depth integrated down- and cross-slope momenta, $m_x = hu$ and $m_y = hv$. With the vector of conservative variables, $\boldsymbol{w} = (h, m_x, m_y)^{\mathrm{T}}$, the model equations (2.1)–(2.3) can be rewritten in conservative form as

$$\frac{\partial \boldsymbol{w}}{\partial t} + \frac{\partial \boldsymbol{f}(\boldsymbol{w})}{\partial x} + \frac{\partial \boldsymbol{g}(\boldsymbol{w})}{\partial y} = \boldsymbol{s}(\boldsymbol{w}). \tag{3.1}$$

The down-slope and cross-slope momentum flux vectors $\boldsymbol{f}$ and $\boldsymbol{g}$ and the vector of the source terms $\boldsymbol{s}$ are given by

$$\boldsymbol{f} = \begin{pmatrix} m_x \\ m_x^2/h + \beta_x h^2/2 \\ m_x m_y/h \end{pmatrix}, \quad \boldsymbol{g} = \begin{pmatrix} m_y \\ m_x m_y/h \\ m_y^2/h + \beta_y h^2/2 \end{pmatrix}, \quad \boldsymbol{s} = \begin{pmatrix} 0 \\ h s_x \\ h s_y \end{pmatrix}. \tag{3.2}$$

The terms β_x and β_y, defined in (2.4), incorporate the extending and contracting states of the avalanching mass through the active and passive earth pressures. Similarly, the source terms s_x and s_y, described in (2.5) and (2.6), are of crucial importance as they include the total driving force generated by gravity, friction, curvature, torsion and local details of the basal topography through its gradient terms. They jointly determine the dynamics of the flow.

We do not further elaborate here on the TVD techniques and optimal choices of limiters and cell reconstructions. Pudasaini (2003) and Wang *et al.* (2004) made a careful study investigating its optimal use in avalanche studies using the Gray *et al.* (1999) version of the SH-equations, and the decision made there will be made here. Finally, we should also mention that different methods, e.g. using the Riemann solver (Koschdon & Schäfer 2003) or the wave propagation method (Vollmöller 2004), have also been successfully applied to the extended SH-equations.

4. Avalanche motion down curved and twisted channels

The model equations (2.1)–(2.3) predict the flow of an avalanche over a non-uniformly curved and twisted channel in which the cross-slope curvature (or the channel width) may equally be varying. The focus is the numerical simulations of such flows, their physical explanation and the analysis and interpretation of

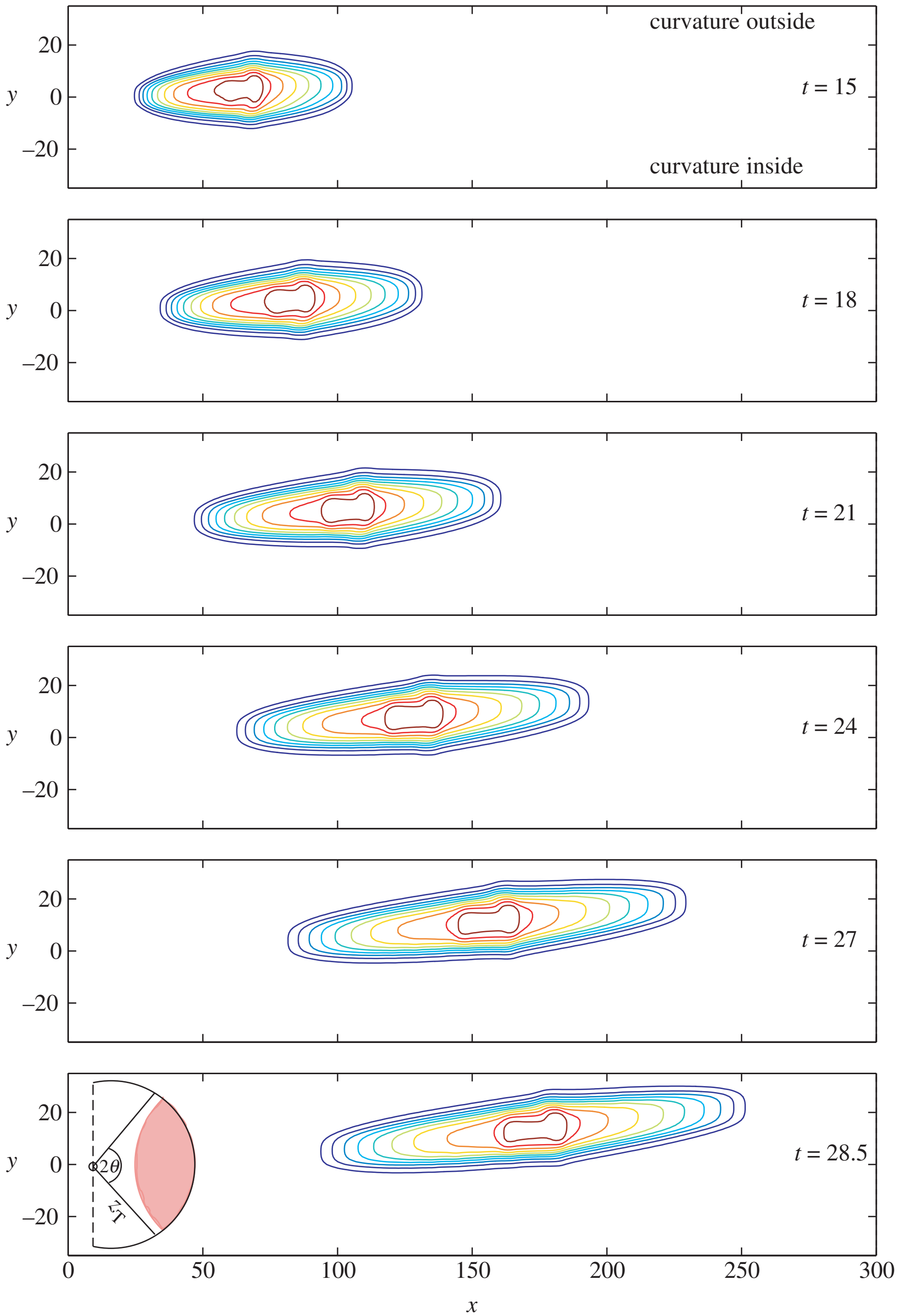

Figure 2. Height contours of an avalanching motion in a helically curved and twisted channel with uniform curvature and torsion and a constant circular cross-slope channel width. The plane rectangles are in reality helically curved and twisted in the x-direction and circularly curved in the y-direction. The inset in the last panel shows schematically the circular cross-section and a cross cut of the avalanching mass.

the results. The main target is the analysis of the joint effects of curvature, torsion, cross-slope topographic variation and 'centrifugal' force in the dynamics of an avalanching body down more general channels and topographies. The form of the employed master curve and the variations of the cross-sections are still somewhat academic or idealistic. This is so because some of them are also used in our laboratory for experiments, but also because the general purpose programme that is applicable to a realistic mountain corrie is not yet ready. Nevertheless, the examples will demonstrate the new aspects that these model equations can disclose, effects that are quantitatively well understood but could, qualitatively, so far not be disclosed. The results will allow us to judge the applicability of the new model equations. On the other hand, they will open a wide spectrum of possibilities for the practitioners involved in the hazard mapping, risk management and public safety. This will then lead to the implementation of the theory into realistic mountain topography, together with GIS elevation data of some specific mountain subregions.

(*a*) *Flows through uniformly curved and twisted channels*

As a first example, we consider a helically curved and twisted channel. This is an academic *test example*, but there are many industrial applications of granular flows in process engineering scenarios where such flow configurations are practically used. For this reason, we consider a *helix* as a master curve so as to form a helically curved and twisted channel. Let us consider a circular helix described by

$$\boldsymbol{R}(\vartheta) = (A\cos\vartheta,\ A\sin\vartheta, -B\vartheta), \tag{4.1}$$

where ϑ is the azimuthal angle. The length, curvature, torsion and pitch of the helix are given by

$$x = (A^2 + B^2)^{1/2}\vartheta, \quad \kappa = A/(A^2 + B^2), \quad \tau = -B/(A^2 + B^2), \quad \mathscr{P} = 2\pi B, \tag{4.2}$$

respectively. Based on the master curve (4.1), a helically curved and twisted channel is formed. The lateral section of the topography is the intersection of a plane perpendicular to the talweg of the channel and the channel itself. Here, this section is a circular arc, but note that when dealing with variable channel widths, the curvature of this arc changes with the width of the channel.

One expects that the flowing granular mass will deviate continuously outward from the central line (i.e. the talweg) of the channel due to the radial acceleration induced by the slope-fitted curvilinear coordinates. Figure 2 displays thickness contours of an avalanche sliding down through a helically curved and twisted channel with uniform curvature and torsion given by (4.2) and a constant cross-slope channel width.[1] The parameter values are: $A=300$, $B=300$, so that

[1] All figures shown for helical chutes are geometrically distorted. The graphs are vertical projections of the chute and granular heaps whose circular–annular geometry are stretched to become straight. Thus, a segment of the annular ring becomes a rectangle of which the top edge is the chute outside and the bottom edge the chute inside boundary. This graphical representation is chosen because it is relatively easy to programme.

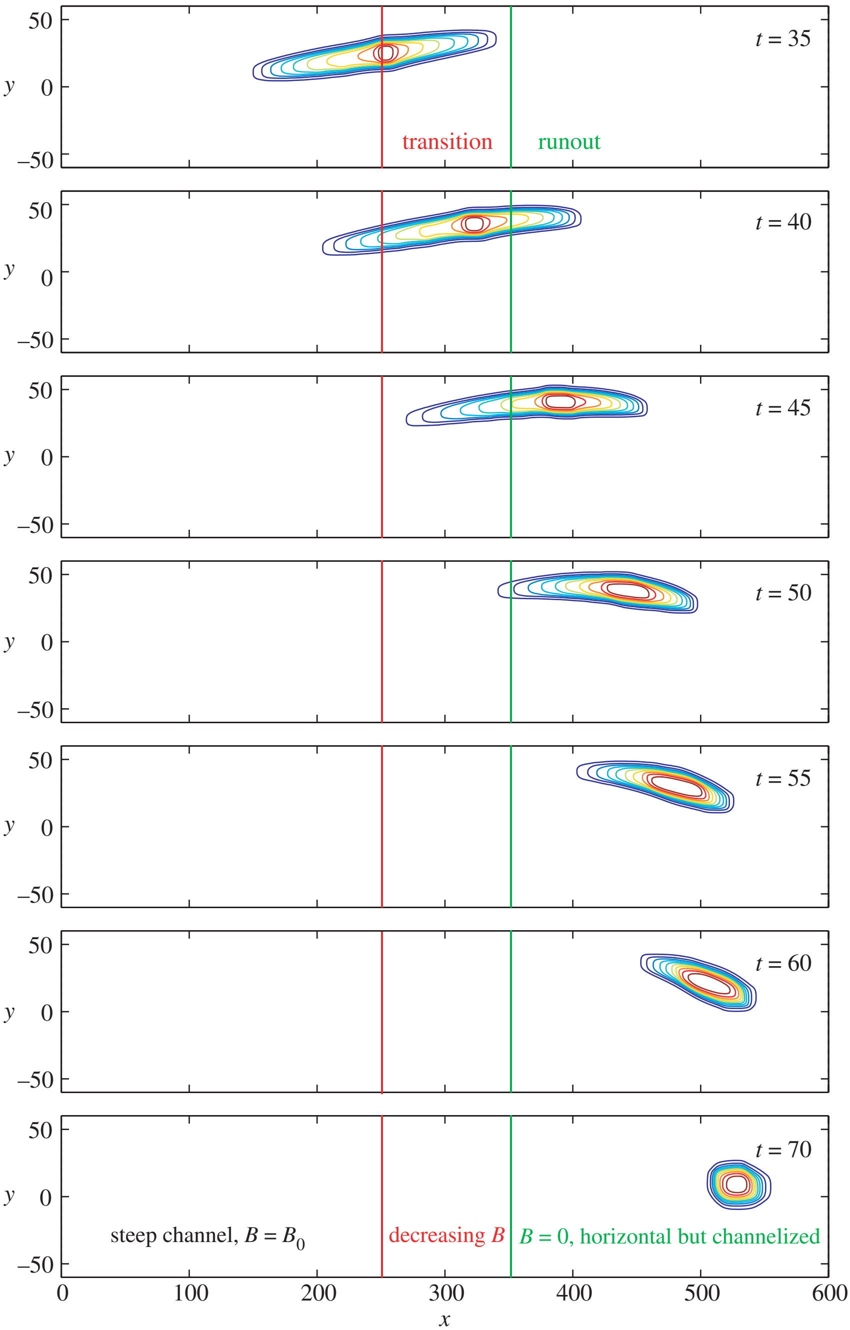

Figure 3. Height contours of an avalanching motion down a helically curved and twisted channel with variable pitch and a constant circular cross-slope channel width.

the channel is inclined relative to the horizontal at 45°; the internal and bed friction angles are $\phi=33°$ and $\delta=27°$, respectively. The radius of curvature in the cross-slope direction is $z_{\mathrm{T}}=128$ and $\theta\in(-44.8°, 44.8°)$ corresponding to $y\in(-100, 100)$. The mass held initially by a hemi-spherical cap centred at $(23, 0)$ with radius 6.5 is suddenly released with zero initial velocity. The contours are plotted at the time-steps 15, 18, 21, 24, 27, 28.5, respectively, only in the vicinity of the flow domain where the granular mass occupies a subregion of it. We also adopt this idea for the plotting of the consecutive figures. As time increases, the avalanching mass is laterally getting less spread, but, it is rapidly moving outwards from the centre line of the channel in the front much more than in the back. This is so because the speed of the front is much greater than that of the tail. Such behaviour of the deforming mass is the joint effect of the curvature, torsion and the radial acceleration that is modelled in the theory (equations (2.1)–(2.3)) through the gravitational acceleration components g_x, g_y, g_z, and the net driving force components s_x, s_y, that include the curvature and torsion of the talweg, bed topography and the cross-slope curvature of the channel. The mass is always extending and accelerating in the down-slope direction, because the channel does not merge into transition- and run-out-zones. In the sequel, we will deal with cases in which the transition and run-out zones are included in the geometrical part of the model.

(*b*) *Avalanching flows through non-uniformly curved and twisted channels*

In reality, channels may be arbitrarily curved and twisted with variable cross-slope curvature and channel width. In particular, realistic avalanche tracks go from steep to flat regions, and on these, the avalanches come to a halt. The geometry must play a crucial role to make the body stand still. The concave curvature of the mountainside increases the bed friction and consequently forces the avalanche to slow down and eventually come to rest. In this subsection we will present avalanche simulations through more general channels that possess run-out zones.

(i) *Variable pitch*

One geometric model is such that the pitch defined in (4.2) can be modified as

$$B(x) = \begin{cases} B_0, & 0 \le x \le x_{\mathrm{l}}, \\ B_0 \left(\dfrac{x_{\mathrm{r}} - x}{x_{\mathrm{r}} - x_{\mathrm{l}}} \right)^2, & x_{\mathrm{l}} \le x \le x_{\mathrm{r}}, \\ 0, & x \ge x_{\mathrm{r}}, \end{cases} \tag{4.3}$$

so that prior to the left end point, x_{l}, of the continuous transition zone, the chute is exactly the same as that used in the previous subsection. However, there is a continuous decrease of the pitch from x_{l} to x_{r}. Then, for $x \ge x_{\mathrm{r}}$ the pitch is always zero, and thus, the subsequent channel is forming a channelized circular run-out. Of course, physically this can only be realized, if $(x_{\mathrm{final}} - x_{\mathrm{r}}) < 2\pi A$, where x_{final} is the end point of the talweg in the run-out zone.

Avalanche simulations for this case are presented in figure 3. The chosen parameter values are as in figure 2, and $B_0 = 300$, $x_{\mathrm{l}} = 250$ and $x_{\mathrm{r}} = 350$. The different forms in figure 3 are presented only for the time slices after the avalanche entered the transition zone. Prior to that, the flow is the same as those displayed in figure 2 ($t = 15$–28.5). Since the pitch of the channel is continuously decreasing for $x > x_{\mathrm{l}}$, from $t = 35$ onward, the granular

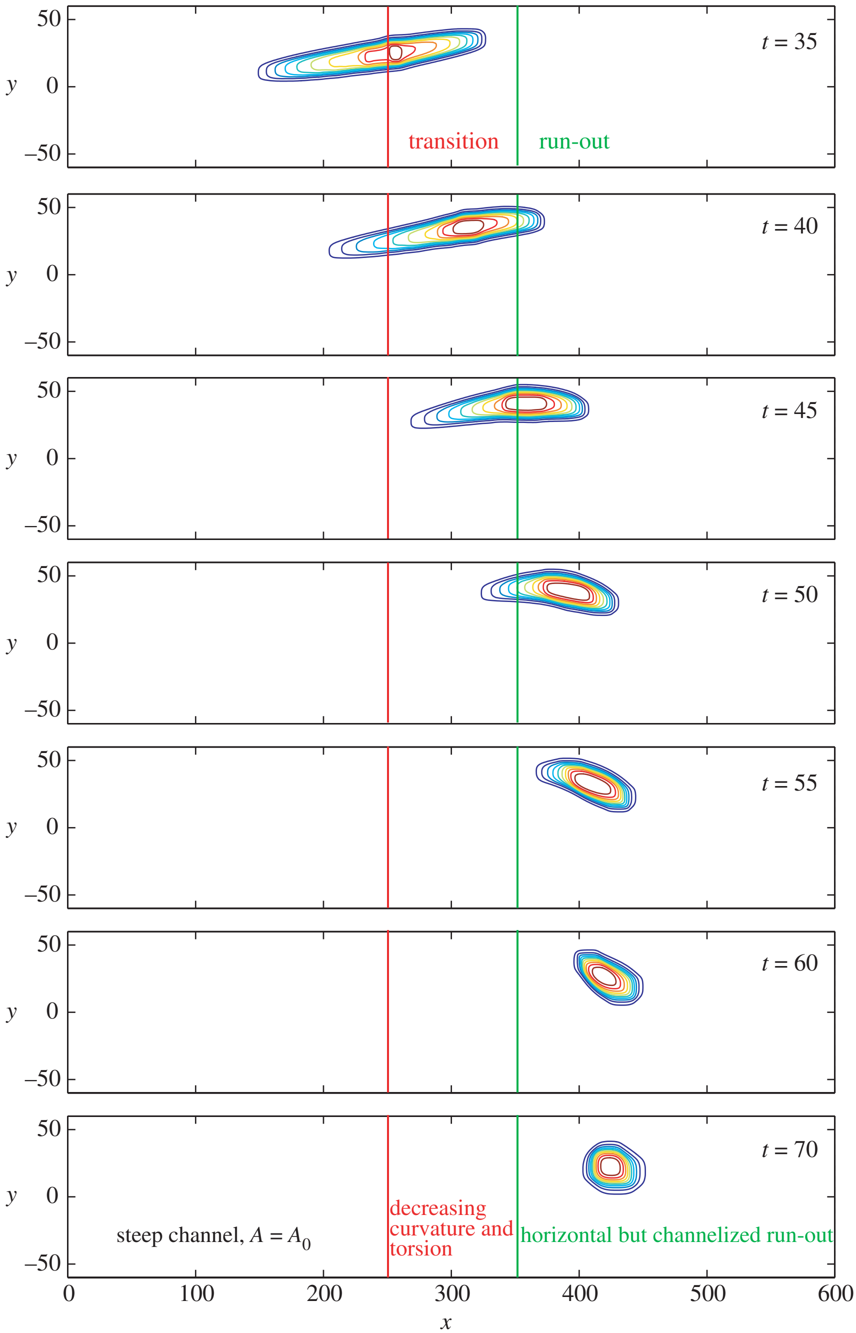

Figure 4. Height contours of an avalanching motion in a helically curved and twisted channel with decreasing curvature and torsion and a constant cross-slope channel width.

mass tends to slow down and turn smoothly towards the central line of the channel. Corresponding to the decrease of the pitch, the inclination angle of the chute with the horizontal plane is also continuously decreased. Ultimately, the channel merges into a horizontal circularly curved channel, thus forming a gully type channelized run-out zone. Beyond $t=28.5$ (figure 2) the sidewise pressure from the channelized bed topography exceeds the force due to the radial acceleration. This happens more effectively at the front than in the rear part, because the velocities are now smaller there than in the rear part. It leads to a continuous rotation of the body towards the centre of the channel. This sidewise pressure is so strong that after $t=60$ the mass crosses the talweg of the channel and heads towards the opposite side of the channel. Finally, the body comes to rest at time $t=70$.

(ii) *Variable curvature and torsion*

Next, consider a channel of which curvature and torsion are redefined with a new expression for A in (4.2) as follows:

$$A(x) = \begin{cases} A_0, & 0 \leq x \leq x_1, \\ A_0 \exp[(x-x_1)^a], & x_1 \leq x \leq x_r, \\ A_0 \exp[(x_r - x_1)^a], & x \geq x_r, \end{cases} \tag{4.4}$$

where a is an exponent that determines the intensity of decrease of the curvature and torsion. For the simulations, we have set $a=1$ and $A_0=300$ so that before the transition $(x<x_1)$ the channel is the same as in the previous case (figure 3). Equation (4.4) tells us that the radius of curvature and the torsion of the channel increase rapidly as the arc-length x becomes larger than x_1. Before this transition point, the channel has uniform radius of curvature, torsion and pitch. This increase forces the channel quickly to merge (approximately), with the curve gradually decreasing until it eventually becomes a horizontal channel. This horizontal portion of the channel also forms the run-out zone for the avalanche.

The results of the avalanche simulation for this configuration are presented in figure 4. There are great differences in the avalanche motion between figures 3 and 4, particularly in the run-out zones. For the present case, since the radius of curvature and torsion increase rapidly from $x=x_1$, the avalanche quickly turns back to the central line of the channel and suddenly comes to rest, much earlier and much closer to the transition zone than in figure 3. It is also interesting to observe that in figure 4, between $t=60$ and 70 the deposit still seems to spread slightly in all directions.

The differences manifest themselves for $t>35$. In particular, for $t=40$, the pile in figure 3 has left the transition zone by approximately one-third of its mass, whereas it is still almost inside the transition zone in figure 4. This can physically be understood: the increasing radius of curvature of the channel axis in the transition zone for case mentioned in this section reduces the local slope angle of the channel axis much faster than for case seen in §4*b*(i), so that within the transition zone of the case mentioned in this section, the avalanching mass encounters deposition-prone conditions quicker than the case seen in §4*b*(i). Comparing the deposits for $t \geq 45$ in the two figures shows that the run-out distance of the avalanche mass is greatly affected.

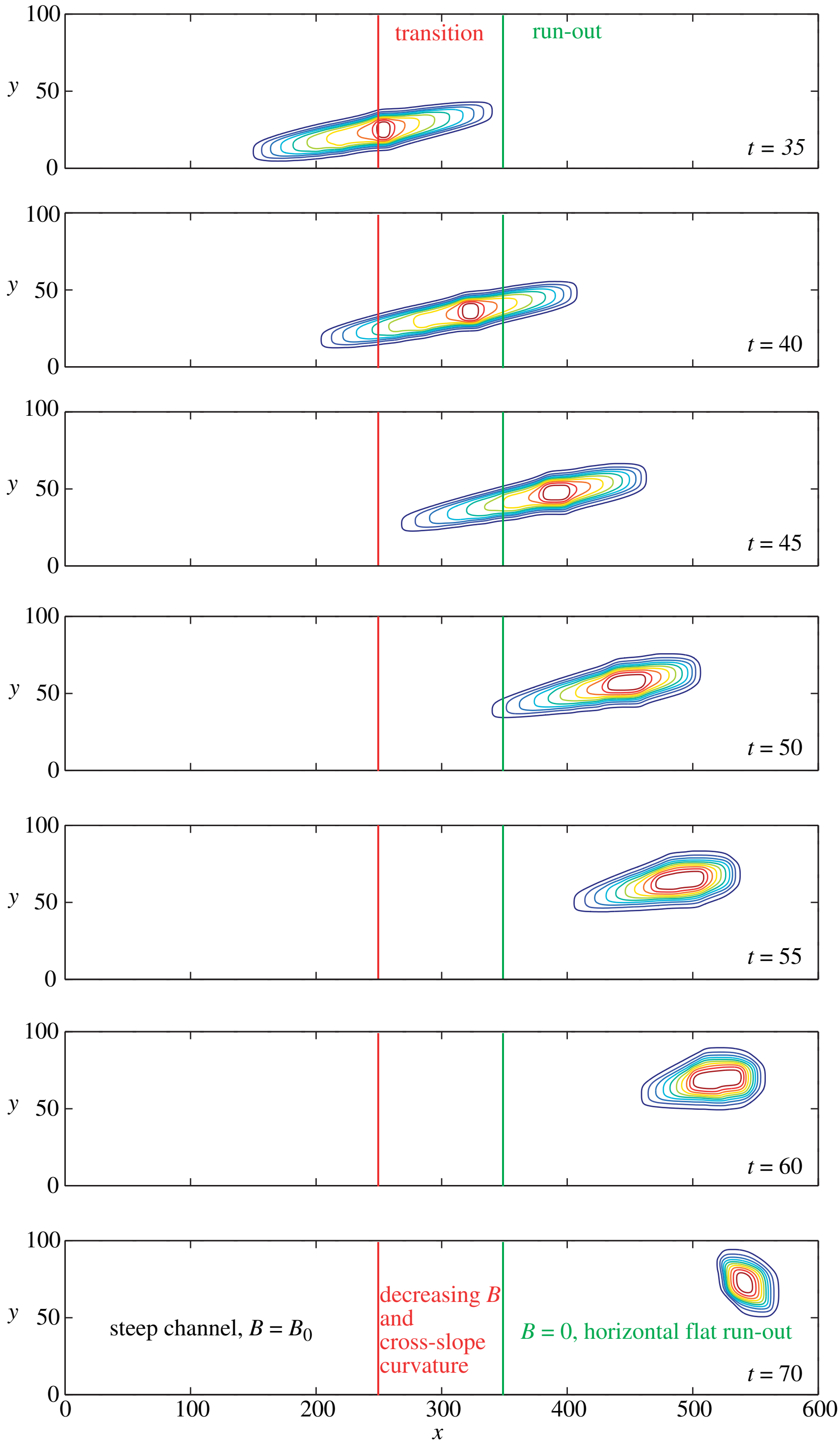

Figure 5. Height contours of an avalanching motion in a helically curved and twisted channel with decreasing pitch and increasing cross-slope channel width.

(iii) *Decreasing pitch and variable cross-slope curvature*

Real channels may be diverging or converging (with respect to their channel width or cross-slope curvature) along the down-hill direction. Therefore, the avalanche theory must be able to deal with more general channels and natural valleys or gullies with generally varying cross-slope curvature. At this point, we simulate the avalanche motion in a channel of which the pitch B, is defined by (4.3), as for the case seen in §4*b*(i), and the parameter A is constant; but now we vary the channel width starting from its left boundary of the transition zone at which the pitch starts to decrease. This can be achieved by defining a channel which merges continuously into an open flat run-out zone according to

$$\theta(x,y)=\begin{cases} y/z_{\mathrm{T}}, & 0\leq x\leq x_{\mathrm{l}} \\ (y/z_{\mathrm{T}})f(x), & x_{\mathrm{l}}\leq x\leq x_{\mathrm{r}}, \\ 0°, & x\geq x_{\mathrm{r}}, \end{cases} \tag{4.5}$$

where z_{T} is the distance between the master curve and the talweg in the upper inclined part of the channel (hence a constant) and $f(x)=(1-(x-x_{\mathrm{l}})/(x_{\mathrm{r}}-x_{\mathrm{l}}))^2$. Thus, the continuous transition of the parametric function θ from its higher value y/z_{T} in the upper part to its zero value in the open run-out zone constitutes a three-dimensional channel that has variable pitch and variable curvature both in the longitudinal as well as in the lateral directions. Figure 5 depicts the contours of the avalanche motion from its transition to the open run-out zone, where only the outward half of the channel is plotted, because in this and the following cases (for $t\leq 35$), the granular masses appear only in this half of the channel. The graphs describe the deformation of the avalanche disclosing the subtle reaction of it to different geometry of the run-out region. Although the pitch is decreasing, after reaching the transition zone the avalanching body is heading radially outwards of the flat run-out zone until it comes to rest close to the outside edge of the chute. The main mechanism for this is that, as soon as the mass enters the run-out zone the radial acceleration decreases rapidly, but, since the chute is flattening in the cross-slope direction, the decreasing radial acceleration must keep the mass further and further away from the centre line. The direction and the process of the deposition is in conformity with our physical intuition and expectation.

(iv) *Decreasing curvature and torsion, and variable cross-slope curvature*

A further interesting geometrical model is a channel of which the curvature and torsion decrease from the beginning of the continuous transition zone as described by equation (4.4). The channel opens and merges continuously into the horizontal plane as described by (4.5) but $B=B_0$ is kept fixed. This case is more important in geophysical applications because curvature and torsion generally decrease as one enters into the horizontal run-out zone of a mountain valley. The avalanching motion from the transition to the run-out zone in such a channel is presented in figure 6. The principal mechanism for the deformation and the deposition of the mass is analogous to case as seen in §4*b*(iii); i.e. figure 5, but it stops earlier in time and at a shorter run-out distance than before. Given the results of cases seen in §4*b*(i) and (ii), this was to be expected.

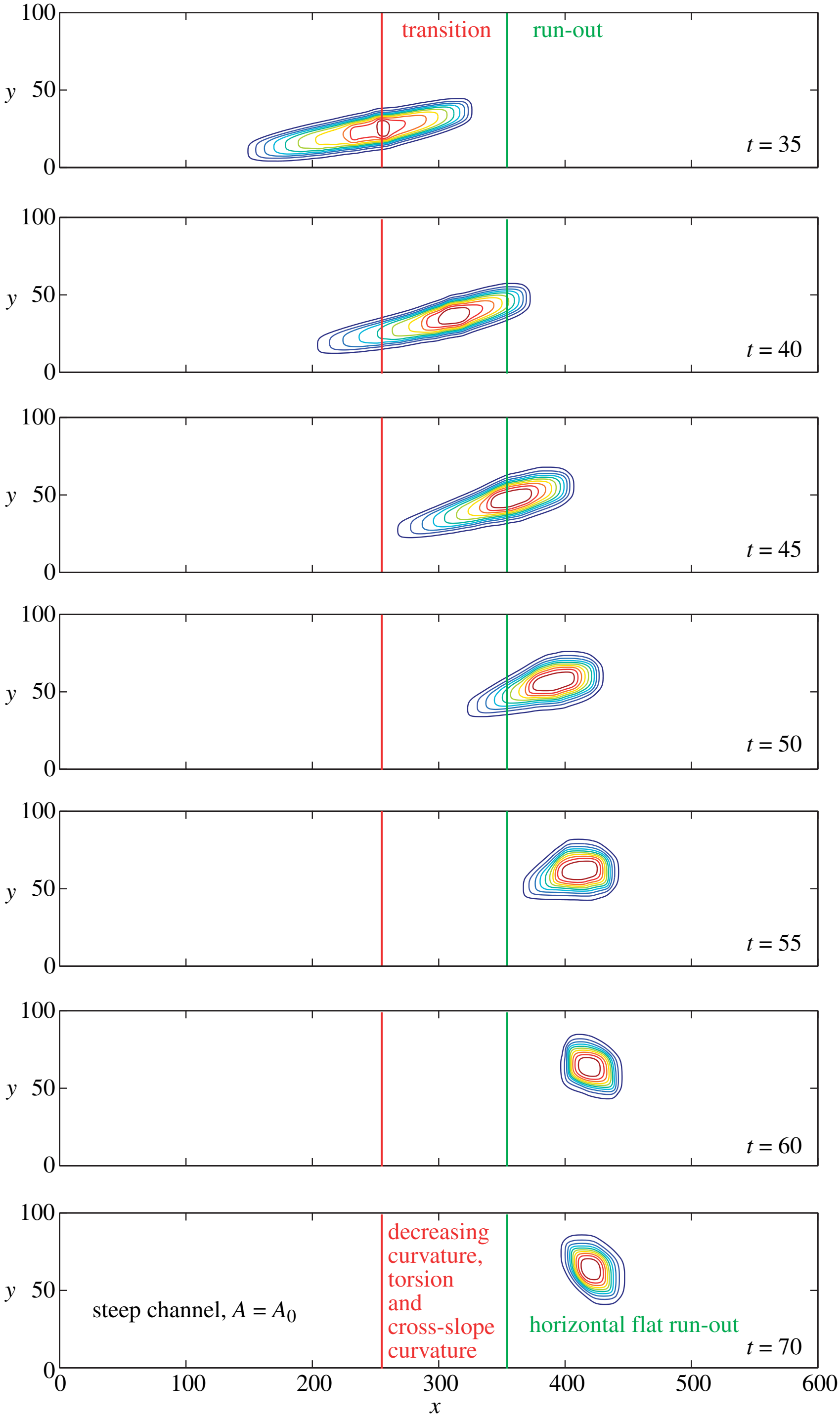

Figure 6. Height contours of an avalanching motion in a helically curved and twisted channel with decreasing curvature and torsion and increasing cross-slope channel width.

5. Concluding remarks

We presented and applied a new model describing the flow of a cohesionless mass of granular materials through curved and twisted channels. The model equations incorporate the simultaneous effects of curvature and torsion of the master curve of the channelized topography systematically in the avalanche motion. This was not possible in the earlier models. The applicability of the present model equations is, therefore, much broader than in previous cases. The advantage of this formulation lies in its flexibility of application. The analysis of the motion of avalanches in channels with different cross-slope curvatures and widths is now possible. The flow down an inclined surface or within a channel with its axis in a vertical plane that may be curved can be described. The examples have shown that the model generates results that are physically expected. The flow down complicated mountain valleys with arbitrarily curved and twisted talwegs and varied bed topographies can genuinely be predicted by these model equations. The geometries are only restricted by the fact that they are not strongly curved and twisted, but a split from a single mass in a corrie to two masses along two different tracks is in principle possible to be described. Thus, the theory provides new directions in the quality of predictions in the field of avalanche and debris flow research. It also opens a large spectrum of applications in different geophysical problems connected with the use of GIS and digital elevation data.

To avoid any spurious oscillations and to include naturally induced shock phenomena into the solution of the nonlinear hyperbolic model equations, with possible discontinuities in the unknown variables and coefficients, we implemented two-dimensional high-resolution NOC shock-capturing numerical schemes with TVD limiters. One of the most basic and fundamental questions related to the new theory is: are these model equations really able to predict flows in chutes and channels that simultaneously incorporate curvature, torsion and the cross-slope curvature effects of the bed topography? To answer this question, several numerical tests were performed for avalanching masses down curved and twisted bed topographies. Uniformly and non-uniformly curved and twisted channels, as well as channels that incorporate continuous transition zones merging into the horizontal run-out zones are considered. Both confined and unconfined transition zones, with constant and variable inclination angles of the topography, are taken into account. Computational findings clearly demonstrate the combined effects of curvature, torsion and the radial acceleration associated with the bed topography. Such sophisticated studies have not been carried out before.

This research was supported by Deutsche Forschungsgeminschaft through the project Hu 412/33-1: *Avalanche Dynamics in Complex Topography*. This manuscript was written while K.H. was a member of the programme *Granular and Particle Laden Flows* at the Isaac Newton Institute at Cambridge University, UK, and while S.P.P. and K.H. were in the satellite workshop at Bristol organized by the INI. The authors acknowledge the constructive reviews by the anonymous referees.

References

Ancey, C. & Meunier, M. 2004 Estimating bulk rheological properties of flowing avalanches from the field data. *J. Geophys. Res.* **109,** F01004.

Denlinger, R. P. & Iverson, R. M. 2001 Flow of variably fluidised granular masses across three-dimensional terrain. 2. Numerical predictions and experimental tests. *J. Geophys. Res.* **106**, 552–566.

Denlinger, R. P. & Iverson, R. M. 2004 Granular avalanches across irregular three-dimensional terrain. 1. Theory and computation. *J. Geophys. Res.* **109,** F01014.

Dent, J. D., Burrel, K. J., Schmidt, D. S., Louge, M. Y., Adams, E. E. & Jazbutis, T. G. 1998 Density, velocity and friction measurements in a dry-snow avalanche. *Annal. Glaciol.* **26**, 247–252.

Eglit, M. E. 1983 Some mathematical models of snow avalanches. In *Advances in mechanics and the flow of granular materials* (ed. M. Shahinpoor), vol. 2, pp. 577–588. Houston, TX: Clausthal-Zellerfeld and Gulf Publishing.

Gray, J. M. N. T., Wieland, M. & Hutter, K. 1999 Gravity-driven free surface flow of granular avalanches over complex basal topography. *Proc. R. Soc. A* **455**, 1841–1874. (doi:10.1098/rsta.1999.0383.)

Gray, J. M. N. T., Tai, Y.-C. & Noelle, S. 2003 Shock waves, dead zones and particle free regions in rapid granular free surface flows. *J. Fluid Mech.* **491**, 160–181.

Grigoryan, S. S. & Ostroumov, A. V. 1977 Mathematical simulation of the process of motion of a snow avalanche (summary only). *J. Glaciol.* **19**, 664–665.

Gubler, H.-U. 1987 Measurements and modelling of snow avalanche speeds. In *Avalanche formation, movement and effects* (ed. B. Salm & H.-U. Gubler), IAHS Publ. 162, pp. 405–420. Wallingford, UK: IAHS Press.

Harbitz, C. B. 1998 Snow avalanche modelling, mapping and warning in Europe (SAME). In *A report of the fourth European framework programme: environment and climate* (ed. C. B. Harbitz). Oslo: Norwegian Geotechnical Institute.

Harten, A. 1983 High resolution schemes for hyperbolic conservation laws. *J. Comput. Phys.* **49**, 357–393.

Harten, A., Osher, S., Engquist, B. & Chakravarthy, R. 1986 Some results on uniformly high-order accurate essentially nonoscillatory schemes. *Appl. Numer. Math.* **2**, 347–377.

Hutter, K. 1996 Avalanche dynamics. In *Hydrology of disaster* (ed. V. P. Singh), pp. 317–394. Dordrecht: Kluwer Academic Publishers.

Hutter, K. & Koch, T. 1991 Motion of a granular avalanche in an exponentially curved chute: experiments and theoretical predictions. *Phil. Trans. R. Soc. A* **334**, 93–138.

Hutter, K. & Rajagopal, K. R. 1994 On flows of granular materials. *Continuum Mech. Thermodyn.* **6**, 81–139.

Hutter, K., Siegel, M., Savage, S. B. & Nohguchi, Y. 1993 Two-dimensional spreading of a granular avalanche down an inclined plane. I. Theory. *Acta Mech.* **100**, 37–68.

Hutter, K., Wang, Y. & Pudasaini, S. P. 2005 The Savage-Hutter avalanche model.: how far can it be pushed? *Phil. Trans. R. Soc. A* **363**. (doi:10.1098/rsta.2005.1594.)

Issler, D. 2003 Experimental information on the dynamics of dry-snow avalanches. In *Dynamic response of granular and porous materials under large and catastrophic deformations* (ed. K. Hutter & N. Kirchner). Lecture Notes in Applied and Computational Mechanics, vol. 11, pp. 109–160. Berlin: Springer.

Iverson, R. M. & Denlinger, R. P. 2001 Flow of variably fluidised granular masses across three-dimensional terrain. 1. Coulomb mixture theory. *J. Geophys. Res.* **106**, 537–552.

Iverson, R. M., Logan, M. & Denlinger, R. P. 2004 Granular avalanches across irregular three-dimensional terrain. 2. Experimental tests. *J. Geophys. Res.* **109,** F01015.

Jenkins, J. T. 2001 Hydraulic theory for a frictional debris flow on a collisional shear layer. In *Continuum mechanics and applications in geophysics and in the environment* (ed. B. Straughan, R. Greve, H. Ehrentraut & Y. Wang), pp. 113–125. Berlin: Springer.

Jiang, G. S. & Tadmor, E. 1998 Nonoscillatory central schemes for multidimensional hyperbolic conservation laws, SIAM. *J. Sci. Comput.* **19**, 1892–1917.

Keller, S., Ito, Y. & Nishimura, K. 1998 Measurements of the vertical velocity distribution in ping pong ball avalanches. *Annal. Clac.* **26**, 259–264.

Koschdon, K. & Schäfer, M. 2003 A Lagrangian–Eulerian finite-volume method for simulating free surface flows of granular avalanches. In *Dynamic response of granular and porous materials under large and catastrophic deformation* (ed. K. Hutter & N. Kirchner). Lecture Notes in Applied and Computational Mechanics, vol. 11, pp. 83–108. Berlin: Springer.

Kröner, D. 1997 *Numerical Schemes for conservation laws.* Leipzeig: B. G. Teubner Stuttgart.

LeVeque, R. J. 1990 *Numerical methods for conservation laws.* Boston, MA: Birkhäuser.

Lied, K. & Bakkehøi, S. 1980 Empirical calculations of snow-avalanche run-out distance based on topographic parameters. *J. Glaciol.* **26**, 165–177.

Lied, K. & Toppe, R. 1989 Calculation of maximum snow avalanche runout distance based on topographic parameters identified by digital terrain models. In *Proceedings of IGS symposium on snow and glacier research relating to human living conditions.* Annal. Glaciol. **13,** 164.

Maeno, N. & Nishimura, K. 1987 Numerical simulation of snow avalanche motion in a three-dimensional topography. *Low Temp. Sci. A* **26**, 99–110.

McClung, D. M. & Lied, K. 1987 Statistical and geometrical definition of snow avalanches runout. *Cold Reg. Sci. Technol.* **13**, 107–119.

McElwaine, J. & Nishimura, K. 2001 Ping-pong ball avalanche experiments. *Annal. Glac.* **32**, 241–250.

Nessyahu, H. & Tadmor, E. 1990 Non-oscillatory central differencing for hyperbolic conservation laws. *J. Comput. Phys.* **87**, 408–463.

Norem, H., Irgens, F. & Schieldrop, B. 1987 A continuum model for calculating snow avalanches. In *Avalanche formation, movement and effects* (ed. B. Salm & H. Gubler), IAHS Publ. No. 126. Wallingford, UK: IAHS Press.

Patra, A. K. *et al.* In press. Parallel adaptive numerical simulation of day avalanches over natural terrain. *J. Volcanology Geotherm. Res.*

Perla, I. P., Cheng, T. T. & McClung, D. M. 1980 A two-parameter model of snow avalanche motion. *J. Glaciol.* **26**, 197–207.

Pitman, E. B., Nichita, C. C., Patra, A. K., Bauer, A. C., Bursik, M. & Weber, A. 2003 A model of granular flows over an erodible surface. *Discrete Contin. Dynam. Syst. B* **3**, 589–599.

Pudasaini, S.P. 2003 Dynamics of flow avalanches over curved and twisted channels: theory, numerics and experimental validation. Ph.D. thesis, Darmstadt University of Technology, Darmstadt, Germany.

Pudasaini, S. P. & Hutter, K. 2003 Rapid shear flows of dry granular masses down curved and twisted channels. *J. Fluid Mech.* **495**, 193–208.

Pudasaini, S. P., Eckart, W. & Hutter, K. 2003*a* Gravity-driven rapid shear flows of dry granular masses in helically curved and twisted channels. *Math. Models Meth. Appl. Sci.* **13**, 1019–1052.

Pudasaini, S. P., Hutter, K. & Eckart, W. 2003*b* Gravity-driven rapid shear flows of dry granular masses in topographies with orthogonal and non-orthogonal metrics. In *Dynamic response of granular and porous materials under large and catastrophic deformations* (ed. K. Hutter & N. Kirchner). Lecture Notes in Applied and Computational Mechanics, vol. 11, pp. 43–82. Berlin: Springer.

Pudasaini, S. P., Wang, Y. & Hutter, K. 2004 Dynamics of avalanches along general mountain slopes. *Annal. Glac.* **38**, 357–362.

Salm, S. 1966 Contribution to avalanche dynamics. IAHS AISH Publ. 69, pp. 199–214.

Savage, S. B. 1989 Flow of granular materials. In *Theoretical and applied mechanics* (ed. P. Germain, M. Piau & D. Caillerie), pp. 241–266. Amsterdam: Elsevier.

Savage, S. B. & Hutter, K. 1989 The motion of a finite mass of granular material down a rough incline. *J. Fluid Mech.* **199**, 177–215.

Savage, S. B. & Nohguchi, Y. 1988 Similarity solutions for avalanches of granular-materials down curved beds. *Acta Mech.* **75**, 153–174.

Tai, Y.C. 2000 Dynamics of granular avalanches and their simulations with shock-capturing and front-tracking numerical schemes. Ph.D. thesis, Darmstadt University of Technology, Darmstadt, Germany.

Tai, Y. C., Noelle, S., Gray, J. M. N. T. & Hutter, K. 2002 Shock-capturing and front-tracking methods for granular avalanches. *J. Comput. Phys.* **175**, 269–301.

Toro, E. F. 2001 *Shock-capturing methods for free-surface shallow flows*. New York: Wiley.

Voellmy, A. 1955 Über die Zerstörungskraft von Lawinen. *Schweizeriche Bauzeitung* **73**, 159–162, see also 212–217, 246–249, 280–285

Vollmöller, P. 2004 A shock-capturing wave-propagation method for dry and saturated granular flows. *J. Comput. Phys.* **199**, 150–174.

Wang, Y., Hutter, K. & Pudasaini, S. P. 2004 The Savage–Hutter theory: a system of partial differential equations for avalanche flows of snow, debris and mud. *ZAMM: J. Appl. Math. Mech.* **84**, 507–527.

Yee, H. C. 1987 Construction of explicit and implicit symmetric TVD schemes and their applications. *J. Comput. Phys.* **68**, 151–179.

Zwinger, T., Kluwick, A. & Sampl, P. 2003 Numerical simulation of dry-snow avalanche flow over natural terrain. In *Dynamic response of granular and porous materials under large and catastrophic deformations* (ed. K. Hutter & N. Kirchner). Lecture Notes in Applied and Computational Mechanics, vol. 11, pp. 161–194. Berlin: Springer.